

Hamiltonian and Lindblad Simulations: Optimization of Trotterization

Rohan Timmaraju,¹ Arun Moorthy,² Brian Zhao,¹ Ethan Kur,³ and Michael Cai¹

¹Columbia University

²Stanford University

³Vanderbilt University

This supplementary file complements the slideshow and github for the MIT iQuHack Quantum Hackathon and is in no way emanating the knowledge presented in those of a paper. We began by using key papers presented in the iQuHack challenge to define and setup the initial problem of optimization of trotterization. From there, we give additional detail about the interesting problems that led us to our final result for our jupyter notebook. From there, we move on to our Task 5 which goes over our own unique tests for trotterization. This last step explores the strengths and weaknesses of trotterization given as a relation to the error, number of shots, and time. We check our solutions with classically evolved models and optimize them for a given objective function. Case studies of different hamiltonians are presented to demonstrate the performance of the optimization algorithm. The analysis aims to identify the specific conditions under which trotterization performs well, offering insights into their parameter usage.

I. QUANTINUUM SIMULATION NOTEBOOK

A. Quantinuum Hamiltonian Simulation Notebook

a. *Task 1* For our first task, we realized that the formula

$$e^{-itX^{(k)}sX^{(k+1)}}e^{-itY^{(k)}Y^{(k+1)}}e^{-it\Delta(Z^{(k)}Z^{(k+1)})}.$$

differs from the definition of TK2 only by a factor of $\pi/2$. Thus, our circuit is given by Figure 1. Note that each term in the diagram should be divided by π . Note also that in later tasks, we often decompose the TK2 gate into XXPhase, YYPhase, and ZZPhase, as TK2 is not a standard gate in other quantum computing libraries.

As stated, the transverse ising model given was

$$H_{\text{Ising}} = -J \sum_{i=1}^{N-1} Z^{(i)}Z^{(i+1)} + g \sum_{i=1}^N X^{(i)}$$

with interaction strength $J = 1.2$ and transverse field strength $g = 1$. To write down the circuit for this term, we decided to interlace the ZZPhase and RX gate together for the ising model as shown in Figure 2. The ZZ Phase gates are ran in an inner loop with angle

$$\theta = \left(\frac{2J}{P} \right) t$$

The gate implements the $e^{-i\theta Z \otimes Z/2}$ operator. The Rx

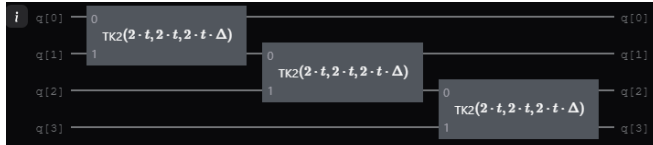


FIG. 1. TK2 Circuit for XXZ Model

gate implements

$$\theta = \left(\frac{2g}{p} \right) t$$

b. *Task 2* Conceptually, we can interpret trotterization as breaking two non-commutative rotations into smaller rotations. As the difference in successive small angle rotations and rotations in the reverse order is a second order term, the trotter error decreases with increasing number of steps.

For higher order trotterization, or second order trotterization, the formula is given by

$$e^{-it(A+B)} = e^{-itA/2}e^{-itB}e^{-itA/2}$$

We can emulate this in the circuit through the first algorithm shown below which simply calculates the trotterization based on the formula given.

Based off of the first and second order trotterization, the error of the statevector is taken to be the difference between the trotterization of a given order and the exact solution given by

$$\epsilon(t) = \| |\psi_{\text{Exact}}(t)\rangle - |\psi_{\text{Trotter}}(t)\rangle \|_{L_2}$$

with our initial value of $p = 1$ to give an error of $\epsilon(1) \approx 0.8$ as shown in Figure 3. This matches our expectations as the 2nd order trotterization should perform better with respect to the number of trotter steps compared to the 1st order.

c. *Task 3* The trotter error is 0 for the initial state $|00\dots00\rangle$. However, when we applied trotterization to the XXZ Model with a different initial state,

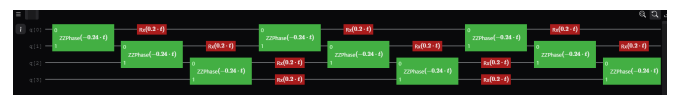


FIG. 2. Transverse Field Ising Model Circuit using Interlacing

Algorithm 1 Generate Trotterized Circuit for the Transverse Ising Model (trotter2)

```

1: procedure TROTTER2( $N, t, p$ )
2:    $J \leftarrow 1.2$ 
3:    $g \leftarrow 1$ 
4:    $circ \leftarrow \text{Circuit}(N)$ 
5:   for  $\text{step} \leftarrow 1$  to  $p$  do
6:     for  $k \leftarrow 0$  to  $N - 2$  do
7:        $circ.\text{ZZPhase}\left(-\frac{J}{p\pi}t, k, k + 1\right)$ 
8:     end for
9:     for  $k \leftarrow 0$  to  $N - 1$  do
10:       $circ.\text{Rx}\left(\frac{2g}{p\pi}t, k\right)$ 
11:    end for
12:    for  $k \leftarrow 0$  to  $N - 2$  do
13:       $circ.\text{ZZPhase}\left(-\frac{J}{p\pi}t, k, k + 1\right)$ 
14:    end for
15:  end for
16:  return  $circ$ 
17: end procedure

```

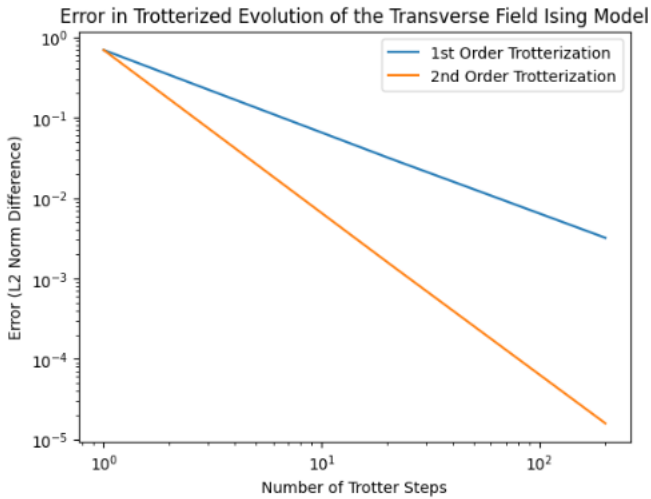


FIG. 3. Error in Trotterized Evolution of Transverse Ising Model

$\frac{1}{\sqrt{2}}(|00\dots00\rangle + |00\dots01\rangle)$, we also observed a converging trotter error (FIG 4). After a prolonged discussion with Eric (Quantinuum), we concluded that the XXZ Model was actually non-commutative. Eric announced this to the other teams later.

Furthermore, when we sort the matrices by their axes instead of by which qubits they apply to, we found a similar converging pattern (FIG 5). Thus, we hypothesize that XXZ is non-commutative for $|00..00\rangle$ too.

d. Task 4 We ran the experiment on a 3-qubit XXZ circuit with initial state $\frac{1}{\sqrt{2}}(|00\dots00\rangle + |00\dots01\rangle)$. We applied a depolarization noise on all CX gates. We chose 2-qubit gate noise over 1-qubit gate noise because it forces the compiler to solve for a device topology, which ensures that the noise is added.

We varied the error probability from 0 to 0.1 and varied

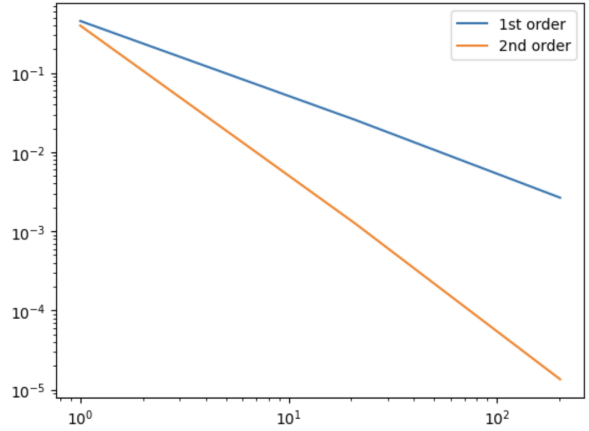


FIG. 4. Error in Trotterized Evolution of XXZ Model, $\frac{1}{\sqrt{2}}(|0000\rangle + |0001\rangle)$

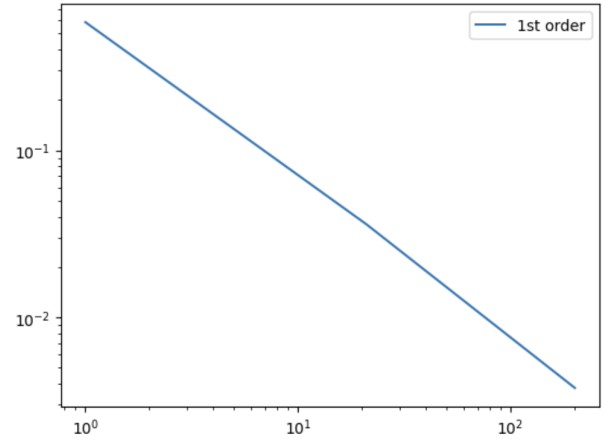


FIG. 5. Error in Trotterized Evolution of XXZ Model, $|0000\rangle$

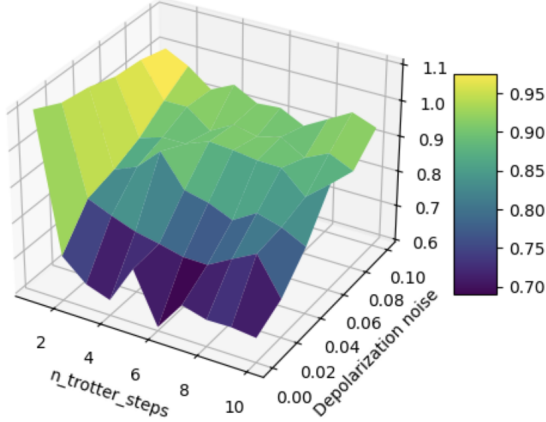
the number of trotter steps from 1 to 10. For each data point, we ran 10 trials, 200 shots per trial, instead of running 2000 shots at once. To understand this choice, we need to differentiate between two types of errors in this experiment.

1. E, the error between the observed outcomes and the expected outcomes of the circuit.
2. The error between the observed E and the expected E.

The aim of the experiment is to investigate how E varies with respect to p. Thus, we want to maximize the first type while minimizing the second type. Both types are reduced by increasing the number of shots, but only the second type is reduced by increasing the number of trials. Ideally, we want to run as many trials as possible, but as each trial is computationally expensive, we capped the number at 10.

Based on the experiments, we made three observations:

Error vs. n_trotter_steps and Depolarization Noise



1. As noise increases, error increases.
 2. The error stops converging above a certain number of steps. This is true even for the noiseless simulation, as the randomness of qubit measurement outweighs any further gain in state vector accuracy.
 3. As the noise increases, the convergence stops sooner.
- e. Task 5 See extension

B. Quantinuum Lindblad Simulation Notebook

a. Task 1 For the first task, we again formulate the initial XXZ Hamiltonian in terms of Pauli operators, in the same way as for the previous task. We then trotterize it to construct the coherent part of the simulation circuit.

$$H_{XXZ} = \sum_{j=1}^{N-1} 2\sigma_+^{(j)}\sigma_-^{(j+1)} + 2\sigma_-^{(j)}\sigma_+^{(j+1)} + \Delta\sigma_z^{(j)}\sigma_z^{(j+1)}$$

$$= \sum_{j=1}^{N-1} X^{(j)}X^{(j+1)} + Y^{(j)}Y^{(j+1)} + \Delta Z^{(j)}Z^{(j+1)}$$

b. Task 2 In task 2, we simulate the dissipative part of the Lindblad evolution by describing the interactions with the environment which evolves from pure states to mixed states. According to the provided formulae, we want to implement the time evolution under the dilated operators K_i for a time of Δt according to

$$\text{tr}_{\text{anc}_1, \text{anc}_2} \left[e^{-i\sqrt{\Delta t} K_1} e^{-i\sqrt{\Delta t} K_2} \left(|0\rangle\langle 0|_{\text{anc}_1} \otimes \dots \otimes |0\rangle\langle 0|_{\text{anc}_2} \right) \times e^{i\sqrt{\Delta t} K_1} e^{i\sqrt{\Delta t} K_2} \right] = e^{\Delta t \mathcal{D}}[\rho] + \mathcal{O}(\Delta t^2).$$

Through dissipative operators and ancilla qubits, we can apply a non-unitary evolution to the main qubits that mimics dissipative dynamics. When building the dilation step, the function `get_dilation_step_deterministic` constructs one trotter step as shown in Figure 6. The two two-qubit gates and ancilla qubits simulate the evolution operators $e^{-i\sqrt{\Delta t} K_{1,2}}$. The dilation angles depend on the dissipative strength (ϵ) and time step (Δt) and are scaled by a factor of $2/\pi$ and $\sqrt{\Delta t}$.

c. Task 3 Next, we wish to perform the full time evolution based on the following equation

$$e^{M\Delta t \mathcal{L}}[\rho] = \left(\prod_{i=1}^M e^{\Delta t \mathcal{D}} \circ \mathcal{U}_{\Delta t} \right) [\rho] \quad (1)$$

with $\mathcal{U}_{\Delta t}[\rho] = e^{-i\Delta t H} \rho e^{i\Delta t H}$.

The code computes $\Delta t = T/M$ and, in each step, appends a coherent evolution block (via `coherent_box`) and a dissipative block (via `dissipative_box_deterministic`) using two ancilla qubits to implement the dilated jump operators. The circuit is initialized with $\rho = |0\rangle\langle 0|^{\otimes N}$.

d. Task 4 In Task 4, we simulate the steady state of the dissipative XXZ Heisenberg model by evolving a small spin chain (e.g., $N = 5$) over a long time ($T = 100$) using $M = 30$ steps. After running the full Lindblad circuit (constructed in Task 3), we measure the Z -expectation value on each qubit:

$$\langle Z^{(i)} \rangle = \text{Tr}(Z^{(i)} \rho),$$

using 300 shots. The measured values are then plotted as a function of qubit index i to produce a spin profile as shown in Figure 7

e. Task 5 In this task, we investigate how varying simulation parameters affects the accuracy and the steady state of the dissipative XXZ Heisenberg model. With a fixed total evolution time T , the time step is $\Delta t = T/M$. As M decreases (i.e., larger Δt), the Trotter error, which scales as $\mathcal{O}(\Delta t^2)$, increases, leading to less accurate results. We explore different values of M to determine the minimum number of steps required for reliable outcomes. Additionally, varying Δ_{ZZ} modifies the ZZ interaction strength in the Hamiltonian, and chang-



FIG. 6. Time evolution and Dissipator Trotterization Circuit

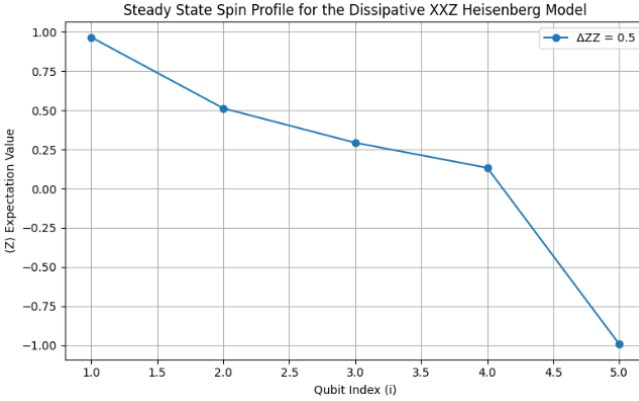


FIG. 7. Steady State Spin Profile for Dissipative XXZ Heisenberg Model

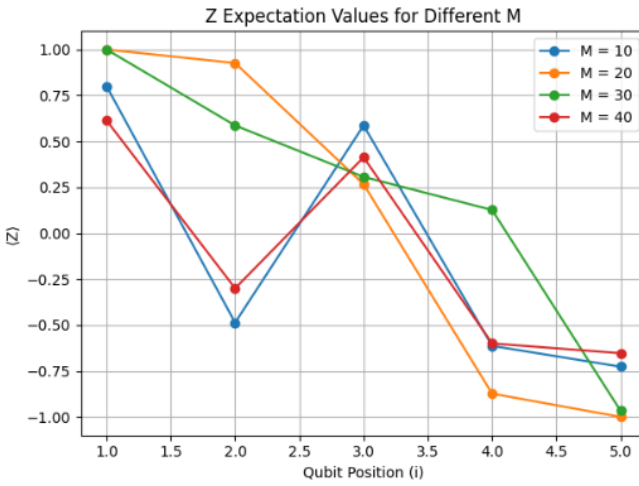


FIG. 8. Z Expectation Values with Different M

ing ϵ (the dissipative coupling) affects the system behavior: large ϵ leads to dominant dissipation, while very small ϵ yields predominantly coherent dynamics.

f. Task 6 In Task 6 we compare the long-time behavior of a spin chain under two types of evolution: the pure Hamiltonian (unitary) and the full Lindbladian (dissipative) dynamics. The Hamiltonian evolution is given by

$$\mathcal{U}(t)[\rho] = e^{-iHt} \rho e^{iHt},$$

which preserves coherence, while the Lindbladian evolution incorporates dissipation, typically described by

$$\frac{d\rho}{dt} = \mathcal{L}[\rho] = -i[H, \rho] + \mathcal{D}[\rho].$$

In our code, two circuits are constructed: one for the Lindblad simulation (including both coherent and dissipative steps) and one for the Hamiltonian simulation only. For $N = 5$ qubits, over a total time $T = 100$ using $M = 30$ steps, the expectation values $\langle Z^{(i)} \rangle$ are measured

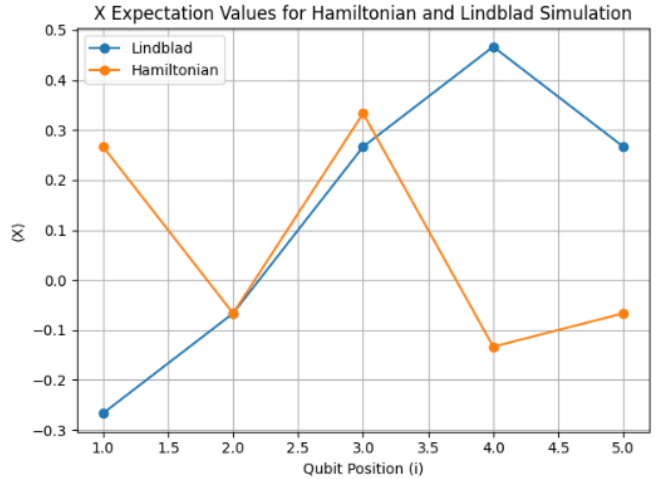


FIG. 9. X Expectation values simulated with the XXZ Hamiltonian and Lindblad simulation

(with 30 shots). These values are then plotted, revealing that while the Hamiltonian simulation exhibits coherent oscillations, the Lindbladian evolution converges to a steady state.

g. Task 7 In Task 7, we study the effect of hardware noise on our quantum simulations by incorporating a noise model into the circuit execution. Specifically, we use a depolarizing error with a small probability (e.g., $p = 0.001$) applied to various single-qubit gates, thereby simulating realistic hardware imperfections. The noisy simulation is then run for both the pure Hamiltonian evolution and the full Lindbladian evolution.

Mathematically, the Hamiltonian evolution is given by

$$\mathcal{U}(t)[\rho] = e^{-iHt} \rho e^{iHt},$$

while the Lindbladian evolution includes dissipative effects:

$$e^{T\mathcal{L}}[\rho] \approx \left(\prod_{i=1}^M e^{\Delta t \mathcal{D}} \circ \mathcal{U}_{\Delta t} \right) [\rho].$$

The results show that under noise the Hamiltonian simulation yields a nearly linear (straight-line) $\langle Z \rangle$ profile, whereas the Lindbladian simulation exhibits a downward trend with the middle qubits displaying more constant values. This behavior reflects how noise, combined with dissipation, drives the system towards a steady state, particularly affecting qubits near the boundaries.

h. Task 8 In Task 8 we implement a randomized version of the dissipative evolution protocol. Instead of deterministically applying both dilated jump operators in each time step, we randomly select one jump operator L_{a_i} and apply the corresponding dissipator \mathcal{D}_{a_i} . This approximates the full evolution,

$$e^{M\Delta t \mathcal{L}}[\rho] \approx \left(\prod_{i=1}^M e^{\Delta t S \mathcal{D}_{a_i}} \circ \mathcal{U}_{\Delta t} \right) [\rho],$$

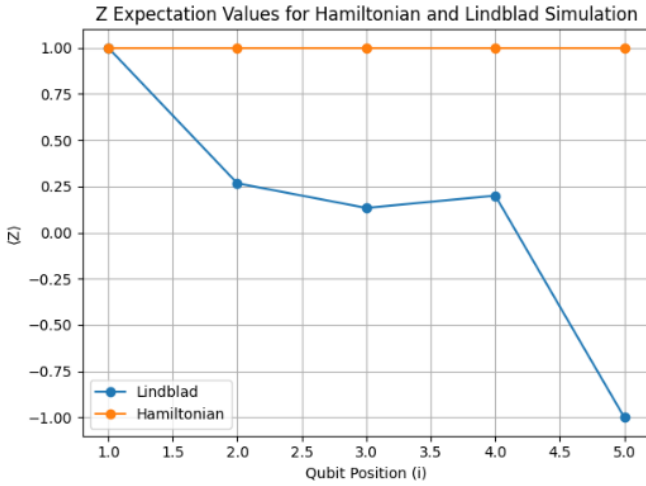


FIG. 10. Z Expectation values simulated with the XXZ Hamiltonian and Lindblad simulation

with

$$\mathcal{U}_{\Delta t}[\rho] = e^{-i\Delta t H} \rho e^{i\Delta t H},$$

and $S = 2$ the number of jump operators. This randomized approach can reduce circuit depth and gate counts, though it may introduce additional statistical fluctuations. In our simulation, the measured $\langle Z \rangle$ profile turned out to be essentially a straight line, indicating a uniform steady state. The plot is labeled with “Qubit Position (i)” on the x-axis and “ $\langle Z \rangle$ Expectation Value” on the y-axis, with the title “Randomized Lindblad Simulation: Z Expectation Values.”

i. *Task 9* We compute the energy evolution of the dissipative XXZ Heisenberg model by first constructing the Hamiltonian

$$H_{XXZ} = \sum_{j=1}^{N-1} \left(X^{(j)} X^{(j+1)} + Y^{(j)} Y^{(j+1)} + \Delta_{ZZ} Z^{(j)} Z^{(j+1)} \right)$$

and obtaining its ground state $|\psi_0\rangle$ via diagonalization. The state $|\psi_0\rangle$ is prepared using a `StatePreparationBox` on an N -qubit register. We then simulate the dissipative dynamics by evolving $|\psi_0\rangle$ with the Lindblad circuit for different evolution times t , and measure the energy expectation

$$E(t) = \langle \psi(t) | H_{XXZ} | \psi(t) \rangle.$$

The resulting energy curve generally trends downward; however, between $t \approx 7$ and $t \approx 16$ the energy exhibits a slight upturn, suggesting transient re-excitation before settling into a steady state.

j. *Task 11*

C. Trotterization Optimizer

We realized that when calculating the trotterization of a given hamiltonian or lindblad, there is going to be

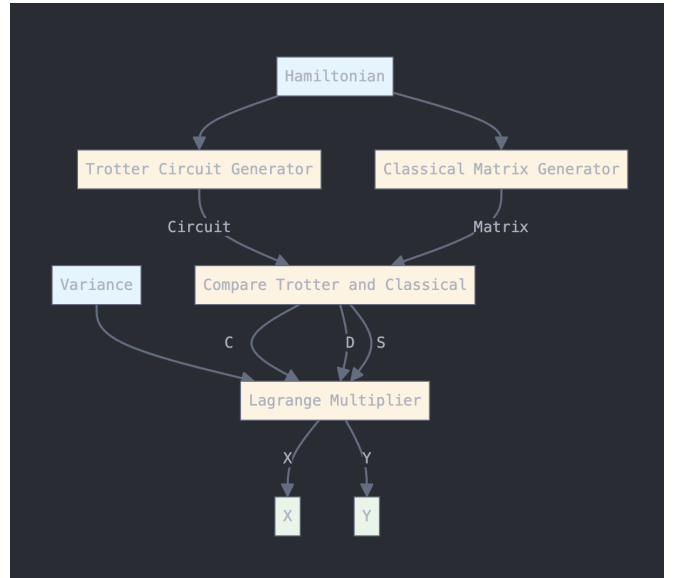


FIG. 11. Flow Chart of Trotterization Optimizer

a tradeoff between accuracy and time, gate depth and noise. In this case, we hope to design an optimization function that helps maximize the accuracy of the trotterization while keeping the time spent on calculations low.

We determine that there are two possible areas to look into which are the costs of computation and the error. For the error, most comes from the trotterization and the noise. For the cost of computation, it comes from the circuit gate depth as well as the number of shots performed to calculate the statevector. Thus, we wish to optimize for the values presented. Thus, our objective function is in the form of

$$J = E + \alpha S p,$$

where:

- E represents the total error, which primarily arises from both the Trotterization approximation and the effects of noise,
- S is the number of shots used to estimate the statevector,
- p is the number of Trotter steps (or evolution steps), and
- α is a scaling factor that quantifies the computational cost per shot and per step.

II. IMPLEMENTATION AND METHODOLOGY

We applied the knowledge learnt through this report for a lightweight trotterization optimizer. Specifically, given an arbitrary Hamiltonian and a desired variance

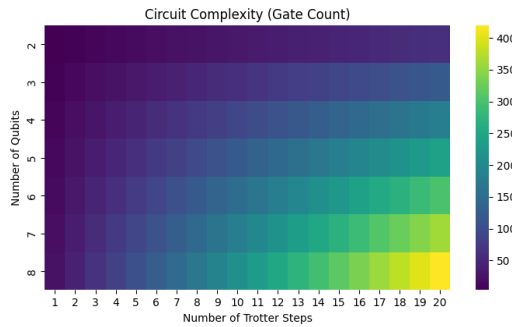


FIG. 12. Total Complexity

V , we aim to output X , the number of shots, and Y , the number of steps, such that the circuit achieves the desired variance, and $X * Y$ is minimized.

Variance consists of random errors from quantum measurement and trotter error.

$$V = \sum \frac{p_i(1-p_i)}{X} + \text{trotter error}$$

Where P and Q are respectively the probability distributions of the trotter circuit's state vector and the ideal state vector. From Section 1 Task 2, we know that trotter error can be expressed as

$$CY^{-D}$$

where C is the error when $Y = 1$, and $-D$ is the gradient of the log-log plot.

Furthermore, we confirmed experimentally that $S = \sum p_i(1 - p_i)$ rapidly converges. Therefore, we can approximate it with a large Y .

We thus have the condition

$$V \geq \frac{S}{X} + CY^{-D}$$

By Lagrange multipliers,

$$X = \frac{S(D+1)}{DV}, Y = \left(\frac{C(D+1)}{V}\right)^{1/D}$$

CODE AVAILABILITY

All code used in this study, including the implementations of trotterization optimizer, is available on GitHub. Interested readers are encouraged to explore the repository to verify results, replicate experiments, or modify the code for further experimentation.

You can access the repository at the following link:

<https://github.com/Rohan-T144/2025-Quantinuum/>

We welcome contributions and suggestions for improving the code. Please feel free to open issues or submit pull requests if you encounter any bugs or have ideas for enhancements.